

PaperID AU491
 Author PRAMESH KUMAR SATAPATHY , OIL AND NATURAL GAS CORPORATION LTD , India
 Co-Authors SUBHANKAR BASU

AN ANALYSIS TO QUANTIFY THE BROADER BANDWIDTH AFTER DEGHOSTING OF MARINE CONVENTIONAL STREAMER DATA

Pramesh Kr Satapathy, Subhankar Basu, SPIC, ONGC, Mumbai
satapathy_pk@ongc.co.in, basu_subhankar@ongc.co.in

ABSTRACT

The broadband data are getting much more importance in structural as well as stratigraphic interpretation and reservoir characterization. Again, the presence of low frequencies adds confidence in building an initial model for inversion. Here the conventional streamer data have been processed in broadband sense to enhance the bandwidth. The deghosting processing step (broadband processing step) requires that the data will be free of swell noise, linear noise, coherent noise, random noise and any anomalous amplitude present in the data. In this paper, we have presented the effectiveness of deghosting during conventional streamer data processing in achieving the broad spectrum. The deghosting step effectively cancels the ghost effects and broadens the spectrum. The outputs of which were analyzed to verify the step. One of the procedures of Quantitative Quality Control (QQC) during Seismic Quality Monitoring (SQM) has been followed for the study. The signal quality of the outputs was compared and subsequently the Bandwidth Index (BI) was quantitatively estimated from the two datasets. In addition, the study was extended to check the impact of broadband processing step at shallow as well as deeper times. The minimum and maximum frequency of the output was shown in terms of octaves and the wavelets are extracted for each octave.

INTRODUCTION

The broadband acquisition and/or processing of marine data is getting popular in the industry due to its advantages in the subsequent stages of exploration. The conventional streamer data is always band limited due to the presence of notches created by reflections from the interface of sea surface and free surface, known as ghost. The ghosts present in the marine data are source ghost which starts its propagation upward from the source, receiver ghost which ends its propagation moving downward at the receiver. They both have the reflections from sea surface, which leads to a reduction of the useful frequency bandwidth and therefore damages the seismic resolution. The sea surface ghost reflection modulate the spectrum of conventional pressure seismic data reducing energy at the so called notch frequencies

$$f_n = nc2z , \quad n = 0, 1, 2, \dots \quad (1)$$

where c is the speed of sound in water and z is the source or receiver depth. As a result of these notches there is a strong loss of useful frequencies in the pressure seismic data.

The ghosts' removal processing stage has been applied to the data to compensate the ghosts' effect and thereby recovering the useful frequencies in the spectrum. The processing stage stretches the frequency band in low as well as higher side of the spectrum. before the ghosts removal are compared, the spectrum of the stack after ghosts' removal shows a considerable broader bandwidth. The increase in

bandwidth increases the resolution of subsurface geological features and the ghost removal enhances the false layering of the subsurface strata.

In this paper we have followed the Quantitative Quality Control (QQC) procedure described by Paternoster et al., 2009, Arman et al., 2014 to Seismic Quality Monitoring (SQM) of wide azimuth data. SQM is the application of a QQC procedure at processing stages to verify and quantify the progress of data processing and to ensure the overall convergence towards the desired data quality. One of the directions, **Signal quality** described in the papers cited above, has been studied for both the outputs before and after deghosting to verify and quantify. The followings are various results that further add to the results derived from QQC procedure.

1. The effect of broadband processing stage has been quantified at different times corresponding to the strong reflectors in the area.
2. The average wavelets extracted from octave outputs were analyzed.

SIGNAL QUALITY

The signal quality monitoring means measuring the signal intrinsic characteristics (amplitude, phase, and frequency content) in either time or Fourier domain at each predefined processing stage. The concept of resolution is closely linked to the seismic maximum frequency and is measured from a scaled version of the autocorrelation time width. However, a seismic data set with a high dominant frequency but narrow bandwidth would carry almost no information. Inversely, a seismic data set with a broad bandwidth represents more interpretation potentialities. Therefore, the seismic bandwidth is a key quality parameter for seismic interpretability. The approach towards seismic bandwidth is based on the time and amplitude characteristics of the autocorrelation function. The ratios, $\Delta T_1/\Delta T_0$ and A_1/A_0 of autocorrelation function (shown in the figure 1) have been measured and plotted to determine the Bandwidth Index (BI) which is a quantitative representation of the bandwidth of the data (shown in the Figure 2). BI is defined as the Euclidian distance between the barycenter of the cloud in the $(\Delta T_1/\Delta T_0; A_1/A_0)$ space and the pole corresponding to the pure sinusoidal case (200%:100%). BI is 0 corresponding to a pure sinusoid waveform and the largest value 141.4 corresponding to a Dirac impulse. In terms of the interpretability, a larger BI reflects the ability of the seismic data set to image real geological interfaces between different rock layers.

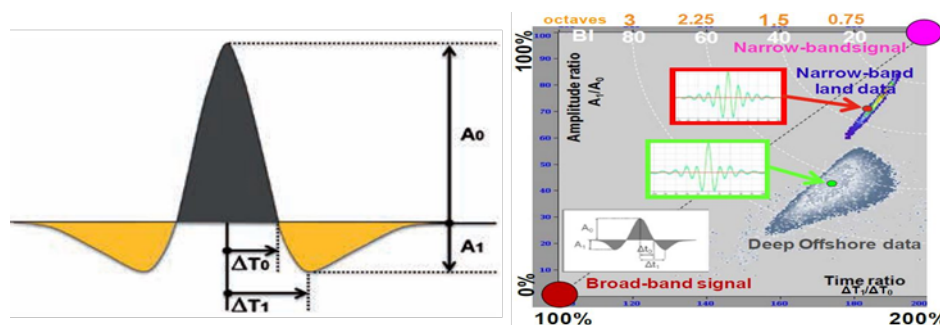


Figure 1: (left) Seismic bandwidth is based on the time and amplitude characteristics of the signal autocorrelation function (Arman et al., 2014), (right) Seismic bandwidth is based on the time and amplitude characteristics of the signal autocorrelation function (Arman et al., 2012)

All the measurements $\Delta T_1/\Delta T_0$ and A_1/A_0 correspond to the autocorrelation function. ΔT_1 is the time difference between the secondary peak (first trough) and the main peak. ΔT_0 is the times difference between the first zero crossing and the main peak. A_1 is amplitude of the secondary peak (first trough) and A_0 is the amplitude of the central peak.

PROCESSING FLOW

The following processing steps (Figure 3) have been applied to the conventional streamer data for preparing outputs for the aforementioned QQC procedure. The stack1 and stack2 (green colored) are the two outputs before and after the broadband processing step respectively. The QQC direction for SQM is followed for the two stacks to disclose the effect of broadband processing stage on the **signal quality** of the data. The signal quality of the two outputs is quantified in terms of bandwidth of the data which has a direct relationship with Bandwidth Index (BI).

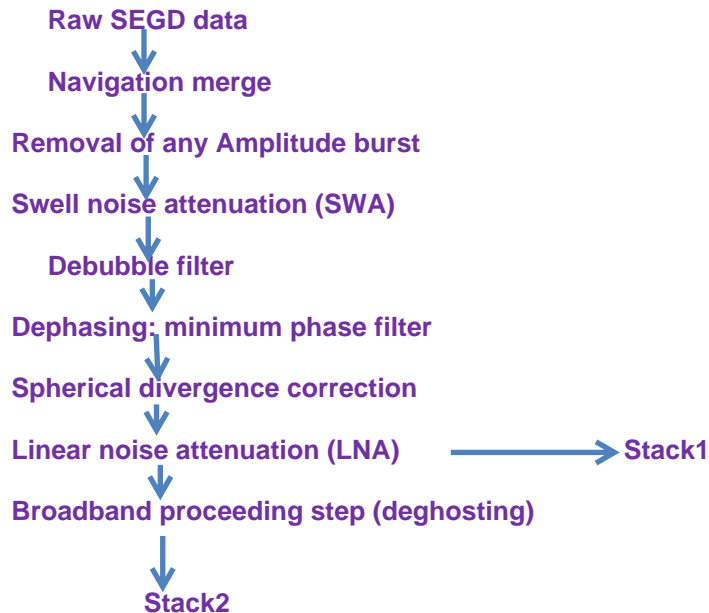


Figure 2: The processing flow followed for the study

METHODOLOGY

The autocorrelation functions (shown in the figures 3 & 4) of both the stacks are calculated by stacking 200 traces in the time window more than 500ms so as to decrease the computation time for the analysis. The functions are computed along three strong reflectors, at 900ms, 2100ms, 2800ms in the area. Then, all the positive numeric values of ΔT_1 & ΔT_0 , A_1 & A_0 are noted for

Figure 3: (left) Autocorrelation functions of stack1 before broadband processing stage and (right) Autocorrelation functions of stack2 after broadband processing stage

RESULTS

The ratio $\Delta T_1/\Delta T_0$ is plotted against A_1/A_0 to calculate the BI for each output under comparison. The BI (see Figure4) of both the outputs are calculated by taking all the attribute values of autocorrelation functions at different times, one at shallower and two at deeper levels of the data. The red color solid circle is the barycenter of the distribution of the attributes of autocorrelation function under consideration (from Arman et al., 2014).

However, the effect of deghosting at different times, shallow and deeper in the data needs to be quantified so that the influence of deghosting at different times' can be evaluated. The BI at different time levels of the data are calculated and shown in the following figures.

Figure 4: (left) The plot between $\Delta T_1/\Delta T_0$ and A_1/A_0 for the stack before deghosting, **BI = 65.19** and (right) the plot between $\Delta T_1/\Delta T_0$ and A_1/A_0 for the stack after deghosting, **BI = 89.02**

Figure 5: (left) the plot between $\Delta T_1/\Delta T_0$ and A_1/A_0 for the stack before deghosting, **BI =56.56** and (right) the plot between $\Delta T_1/\Delta T_0$ and A_1/A_0 for the stack after deghosting, **BI= 72.11** at time 900ms (shallow level)

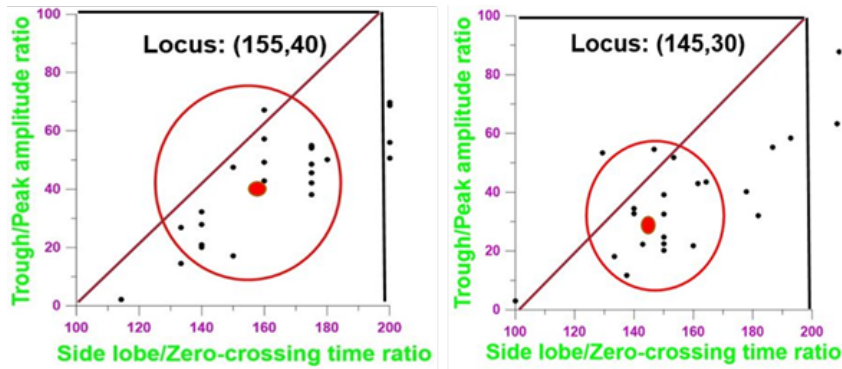


Figure 6: (left) the plot between $1/A_0$ for the stack stage, **=58.30** and (right) the plot between $\Delta T_1/\Delta T_0$ and A_1/A_0 for the stack after deghosting, **BI=89.02** at time 2100ms (deeper level)

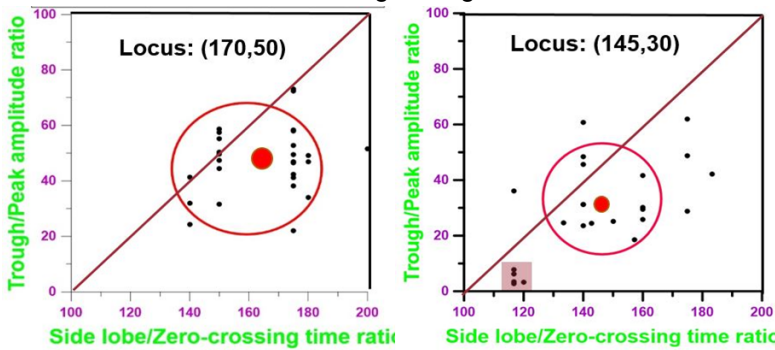


Figure 7: (left) the plot between $\Delta T_1/\Delta T_0$ and A_1/A_0 for the stack before deghosting, **BI =** and (right) the plot between $\Delta T_1/\Delta T_0$ and A_1/A_0 for the stack after deghosting, **BI=** at time 2800ms (deeper level)

SPECTRA ANALYSIS

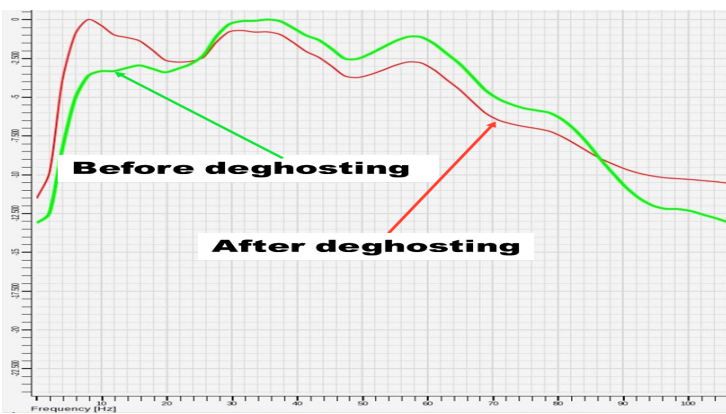


Figure 8: Amplitude spectra of stacks before (red curve) and after deghosting (blue curve). The improved bandwidth at lower as well as higher side. The data has attended a frequency bandwidth of 4-128Hz with 5 octaves.

FILTER PANEL TEST

The output stack of the broadband processing stage has been tested for various band pass filters as shown below in Figure 20. The output could have 5 octaves starting from 4 Hz at the lower side to 128Hz at higher side

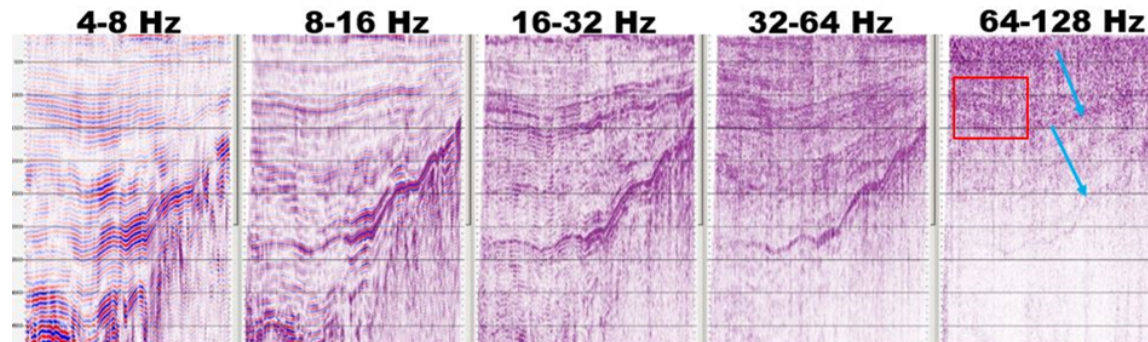


Figure 9: Outputs of various band pass filters (as levelled) applied on the broadband processing stack

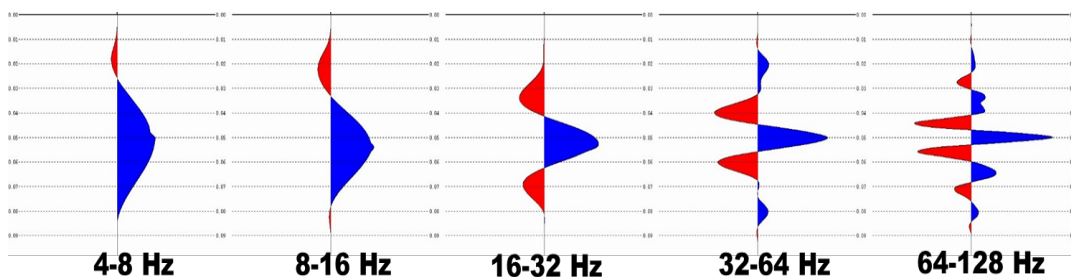


Figure 10: Extracted wavelets from the filter panel outputs

CONCLUSIONS

In this study we have presented a quick analysis (less number of observations of autocorrelation functions, were considered) of the broadband processing stage by following the one of the direction, signal quality, of QQC for SQM and additional QCs are also presented to complete the analysis. The following notes may be outlined from the case study.

1. The overall BI of the output of broadband processing stage is much higher than its counterpart. As the BI has a linear relationship with the bandwidth, the output has attained better quality.
2. The QQC direction has also been extended to check the effectiveness of the processing stage at different times. It may be observed that the data at deeper times have much more benefited due to its higher BI. This could be a reason that deghosting stage improves imaging of the deeper features.
3. The side lobes of extracted wavelet have been diminished after the broadband processing which will add lower frequencies (lower frequencies are boosted as shown in spectrum) to the central lobe. Again, the amplitude spectrum of the wavelet is much likely to be box car which gives better resolution (S24.1, pp 604, SEG, by Harry R. Espey, Geotrans, Inc.). The resolution has been increased as the total area under the frequency spectrum (S24.1, pp 604, SEG, by Harry R. Espey, Geotrans, Inc.) controls the resolution and is increased after broadband processing stage. The convergence towards the broadband spectrum is also superior.

4. The deghosting step results in clearer, sharper and less ambiguous interpretation of final processing outputs in terms of subsurface geology, morphology and stratigraphic features. At the same time it eradicates the false geological layers and structures.

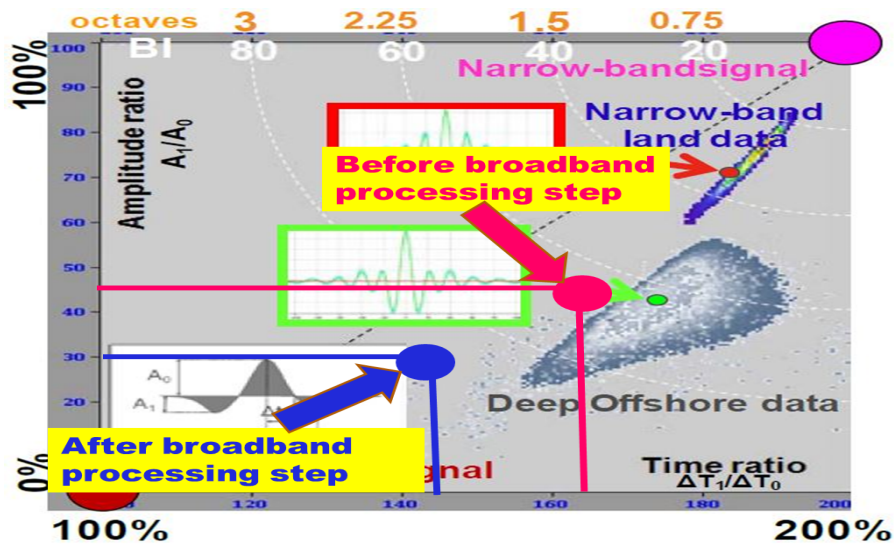


Figure 11: The pink color circle shows the locus of barycenter before deghosting (broadband processing step) and the blue color shows after deghosting.

ACKNOWLEDGMENTS

The authors are grateful to ONGC Ltd.

REFERENCES

- Araman, A., Paternoster, B., Isakov, N., 2012, Seismic quality monitoring during processing: what should we measure? SEG International Exhibition and 82nd Annual Meeting, Expanded Abstracts.
- Araman, A., Paternoster, B., 2014, Seismic quality monitoring during processing: First Break, vol. 32, 69-78.
- Amundsen, L., Zhou, H., 2013, Low-frequency seismic deghosting: Geophysics, vol. 78, no. 2, WA15-WA20.